STEM and STXM-XANES analysis of FIB sections of Ultracarbonaceous Antarctic Micrometeorites (UCAMMs)

B Guérin, C Engrand, C Le Guillou, H Leroux, J Duprat, E Dartois, S Bernard, K Ben- Zerara, J Rojas, M Godard, et al.

STEM and STXM-XANES analysis of FIB sections of Ultracarbonaceous Antarctic Micrometeorites (UCAMMs). B. Guérin[1], C. Engrand[1], C. Le Guillou[2], H. Leroux[2], J. Duprat[1], E. Dartois[3], S. Bernard[4], K. Benzerara[4], J.Rojas[1], M. Godard[1] , L. Delauche[1], D. Troadec[5].
[1]Université Paris-Saclay, CNRS, IJCLab, 91405, Orsay, France (baptiste.guerin@csnsm.in2p3.fr), [2]UMET, CNRS/Univ. Lille, 59655 Villeneuve d'Ascq, France, [3]ISMO, CNRS/Univ. Paris Saclay, 91405 Orsay Campus, France, [4] IMPMC, CNRS/Sorbonne Université/MNHN, Case postale 115, 4 place Jussieu, 75252 Paris Cedex 05, France, [5]IEMN, CNRS/Univ. Lille, 59655 Villeneuve d'Ascq, France.

Introduction: Ultracarbonaceous Antarctic Micrometeorites (UCAMMS) are extraterrestrial dust particles containing large amount of carbonaceous material with elevated D/H ratios [1] and high N/C atomic ratio (up to 0.2)[2]. UCAMMS are rare (~ 1% of the particles in the Concordia meteorite collection) but they have been identified in several collection of interplanetary dust [3, 4]. They are most probably of cometary origin. Here, we studied the association of organic matter and minerals by scanning transmission X-ray microscopy (STXM-XANES) coupled with scanning transmission electronic microscopy (TEM/STEM).

Samples and Methods: The UCAMMs studied here were collected in the Antarctic snow, close to the Concordia station at Dome C [3]. FIB sections of 8 UCAMMs (DC06-18, DC06-41, DC06-43, DC06-65, DC06-308, DC06-139, DC16-30, DC16-309) were analyzed using synchrotron based STXM-XANES at the carbon, nitrogen and oxygen K-edges. The FIB sections were subsequently analyzed with transmission electron microscopy (TEM/STEM) using a FEI Tecnai G2 20 and a FEI TITAN Themis 300 [5, 6]. Peak identification of STXM-XANES spectra are based on [7]. XANES spectra are processed and quantified using Quantorxs method [8] and quantification of STEM EDS spectra has been realized using Hyperspy software [9]. Here, we mainly present results obtained on two recently identified UCAMMs (DC06-308 and DC16-309) and compare them with previous observations [1, 5, 6].

Results: The STXM-XANES analysis reveals 3 types of organic matter (OM) characterized by different carbon speciation. Figure 1 shows type I OM in blue and type II OM in green, both having spectra close to that of chondritic insoluble organic matter (IOM). The main peaks of type I and II OMs are found around 284.8 eV (aromatic and olefinic groups (C=C)), 286.4 eV (ketone and phenol C=O) and 288.4 eV (carboxyl O=C-O). Type II OM exhibits similar functional groups as type I OM but the first peak position is shifted to 285 eV, indicating a stronger contribution of the aromatic groups. The atomic N/C ratio of types I/II OMs range between 0.01 and 0.05 (1σ=0.02) similar to those of chondritic IOM. The type III, in red on Figure 1 exhibits larger differences. The main peak is at 286.4 eV (C≡N nitrile), a small peak at 284.8 eV (alkene C=C) is visible, and the spectra do not exhibit dominant oxygen-related peaks although a limited C=O absorption contribution to the observed absorption continuum may be present. The atomic N/C ratios for type III OM are higher (0.07<N/C<0.2) than in type I and II OMs. The three types of OM are not systematically present in the same section although type I and II are often associated to each other, as described in [5, 10].

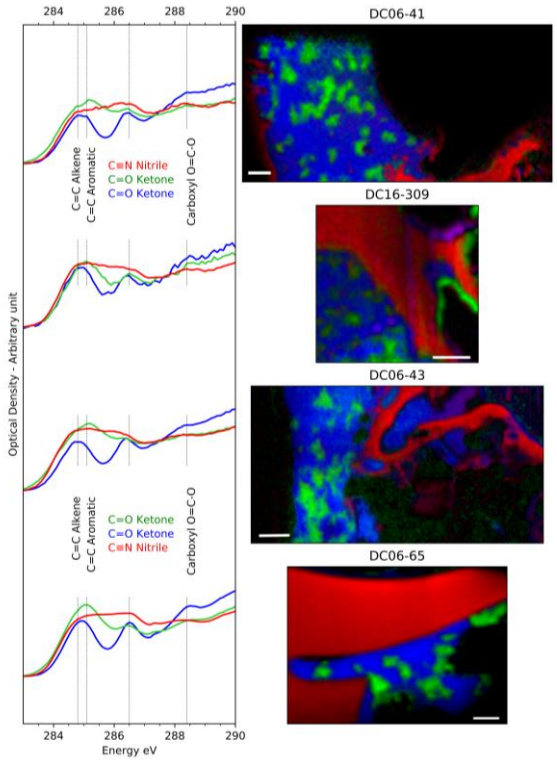

Figure 1: (left) C-XANES spectra of selected UCAMM FIB sections obtained by spectral deconvolution of hyperspectral STXM-XANES maps. (right) Corresponding OM types displayed in false color images (type I: blue, type II: green, type III: red). Scale bar corresponds to 1µm.

Four of the FIB sections (DC06-43, DC06-18, DC06-308 and DC16-309) contain small refractory mineral assemblages embedded in abundant carbonaceous matter. Some are fully crystalline, others are hypocrystalline (mixture of amorphous silicate and crystals) and some are amorphous phases. Crystalline mineral assemblages are only present in type I OM (in

blue, Fig. 1) and consist mainly of Mg-rich pyroxenes (DC16-309, DC06-308, DC06-43, DC06-18), olivines (DC06-18, DC06-43, DC16-309), low-Ni Fe-sulfides (atomic Ni/Fe<0.05) and Fe-oxides [see also 5,11]. Pyroxene grains are more abundant than olivine, with a pyroxene/olivine abundance ratio larger than unity for most UCAMMs [11]. These crystalline phases can be decorated with low-Ni Fe-sulfides and Fe-oxides, with size ranging from tens of nm to sub-µm located at the edge of primary minerals. Analysis of DC16-309 also revealed a mineral exhibiting a fibrous texture reminiscent of that of a phyllosilicate (Fig. 2a). Its composition is rather close to the chondritic composition but with a high Al/Si atomic ratio (Fig 2). The phyllosilicate is in contact with a mineral assemblage containing pyrrhotites (size >200 nm) and smaller Fe-oxides (tens of nm in size, Fig 2b, 2c).

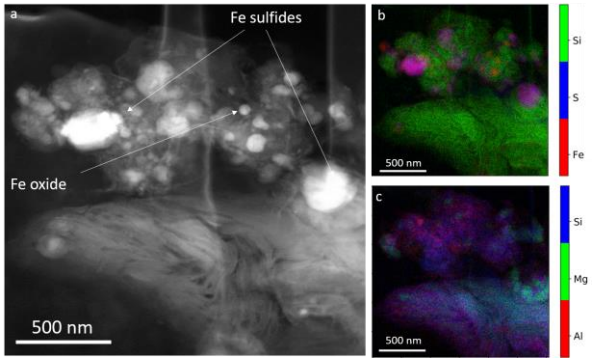

Figure 2: (a) HAADF image of the fibrous structure observed in DC16-309 (b,c) Elemental map based on EDS intensities for Si, S and Fe (b) and Si, Mg and Al (c) .

Hypocrystalline assemblages, already described in [5, 11], are present in one of the new sample (DC06-308). They contain nanometric to micrometric Mg-pyroxene embedded in a SiO_2-rich glass. GEMS (DC06-18, DC06-43, [11]) and GEMS-like (containing larger Fe-sulfide) objects (DC16-309, DC06-308) are present, embedded in types I and III OMs.

STEM-EDX analysis of type II OM in DC16-309 and DC06-308 also revealed that the "patches" in the OM (in green, Fig. 1) contain small amounts of Si, S and a mineral of Na_2SO_4 composition was identified in DC16-309. A small Fe-rich carbonate is also present in DC06-308.

Discussion: C- and N- XANES signatures of the different types of OM suggest that types I/II OMs and type III OM have different origins. Types I/II OMs embed mineral assemblages, and possibly originated from the inner solar system while the N-rich organic matter is devoid of crystalline phases and could have formed by irradiation of N-rich ices in the outer solar system [2, 12]. This indicates that inner solar system components were distributed to the outer solar system through radial mixing in the protoplanetary disk [e.g. 13], to be incorporated in UCAMMs. The presence of secondary phases such as carbonates, and possibly phyllosilicate, suggests possible aqueous alteration of UCAMMs, as proposed by [10], or accretion of mineral components from evolved parents body, as observed for the Wild 2 comet [14]. In the case of in-situ formation, the phyllosilicate in DC16-309 could possibly result from the alteration of GEMS-like object by a basic fluid, conditions which could occur on comets [15]. The formation of large Fe-sulfides and S-rich "dusty patch" (in type II OM) could also result from the interaction with a S-rich fluid. Such alteration may lead to the formation of sodium sulfate (as in DC16-309) and carbonate (as in DC06-308).

Moreover, the presence of Fe-oxides mixed with crystalline silicates and interstitial SiO_2-rich glass phase may point out to a mild heating event (300-400°C) that could have led to the recrystallization and oxidation of a Fe-rich amorphous precursor (possibly GEMS [16]), possibly during atmospheric entry.

The association of these heterogeneous phases confirm the complex history and journey of UCAMMs which are made of materials formed in the hot inner solar system (crystalline phases) associated with OM similar to that of CCs and assembled with colder outer solar system matter (type III OM), along with possible secondary alteration processes or mixing with already processed interplanetary materials.

Acknowledgements: This work is supported by ANR COMETOR, CNRS, Labex P2IO, IN2P3, INSU, Univ. Paris-Saclay, DIM-ACAV and CNES. The micrometeorites were collected at Concordia Station with the support of the French Polar Institute (IPEV).

References:

[1] Duprat, J., *et al.* (2010), *Science*, **328**(5979), 742-745. [2] Dartois, E., *et al.* (2013), *Icarus*, **224**(1), 243-252. [3] Duprat, J., *et al.* (2007) *ASR*, **39**(4), 605-611. [4] Nakamura, T., *et al.* (2005) *MAPS Supp.*, **40**, 5046. [5] Engrand, C., *et al.* (2015), *LPSC* (Vol. 46, p. 1902) [6] Charon, E., *et al.* (2017*), LPSC (*Vol 48, p. 1964*)* [7] Nuevo, M., *et al.* (2011), *ASR*, **48**(6), 1126-1135. [8] Le Guillou, C., *et al.* (2018), *AC*, **90**(14), 8379-8386, [9] F. de la Pena, *et al.* (2019) HyperSpy v1.5.2., [10] Yabuta, H., *et al.* (2017), *GCA*, **214**, 172-19. [11] Dobrică, E., *et al.* (2012), *GCA*, **76**, 68-82. [12]Augé, B., et al. (2016) AA, **592**, A99. [13] Ciesla F.J. and Sandford S.A. (2012) *Science* **336**, 452-454. . [14] Brownlee, D. (2014). *AREPS*, **42**, 179-205. [15] Nakamura-Messenger, K., *et al.* (2011), *MAPS*, **46**(6), 843-856. [16] Bradley, J. P., *et al.* (2014), *LPSC* (Vol. 45, p. 1178).